THERMO-MECHANICAL PROPERTIES OF TRIAXIALLY-WOVEN FABRIC COMPOSITE FOR DEPLOYABLE STRUCTURES

Takahira Aoki*, Keishiro Yoshida and Akihito Watanabe*****
***University of Tokyo, **Kanazawa Institute of Technology, ***Sakase Adtech, Co., Ltd.**

Keywords: *Fabric composite, woven yarns, space structure, isotropic, bending, thermal expansion*

Abstract

Triaxially woven fabric (TWF) composite is made up of three sets of inter-woven tows placed in three equally spaced in-plane directions combined with the matrix resin impregnated in the tows. The bending characteristics of carbon fiber/epoxy TWF composite are analytically and experimentally investigated in this study. The stiffness isotropy observed under tensile loading is shown to hold as well under the flexural loading based on the linear analysis combined with the assumption of infinite size specimens. The effect of specimen width shows up as well under bending analysis. The anisotropy that emerges at high loading levels under tensile load is predicted to be not as salient under the flexural loading. To verify the analytical predictions, pure bending test is conducted. The experimental results support the predicted isotropy for infinite plates, though the actual specimens are of finite width. Thermal loading test is also conducted using rectangular specimens to experimentally obtain the thermal expansion coefficients, which are found to be larger than that predicted previously through the analysis. The overall isotropic nature as well as the excellent flexural strength of the TWF that the material system is one of the potent candidates for various components of light-weight deployable structures, especially in space use.

1 Introduction

Triaxially woven fabric (TWF) constitutes of three sets of inter-woven tows or yarns oriented in equally spaced 0^o, $+120^o$ and -120^o angles within a single plane . The fabric is then impregnated with matrix resin to constitute a single-ply 2-dimensional (2-D) TWF composite. The material system is utilized in various fields, including space structures due to its low apparent density and high flexibility together with the expected isotropy in stiffness, all of these characteristics arising from its distinctive configuration. Low thermal sensitivity of the carbon fiber TWF composite is also advantageous when used in space structures. Therefore, it is of great importance to precisely evaluate the mechanical and thermal behaviors of the TWF composites both theoretically and experimentally. The investigations on fundamental mechanical behaviors [1,2] have revealed that the isotropic nature of the stiffness emerges for infinite plate and the overall experimental results can well be predicted by numerical analyses considering the periodicity of the composite.

In the present study, bending behavior of TWF composite made from carbon fiber tows and epoxy resin are investigated both theoretically and experimentally in order to evaluate the folding characteristics that are essential when the composite is used in the deployable structures. Linear finite element analysis is first conducted for the unit cell region of the periodic structure. The unit cell models are then aligned to analyze the width effect on bending. Nonlinear analysis is performed to investigate the geometrically nonlinear behavior of TWF composite under bending. Thermal loading test is also conducted to verify its applicability to the structures sensitive to the thermal deformations.

2 Description of TWF Composite

The TWF composite used in the study is the combination of T300-1K carbon fibers (Toray Industries Inc.) and 180^oC-cure NM35 epoxy resin

(Nippon Oil Corp.). Dry carbon fabric is first woven to form a TWF and the resin is then impregnated to form a prepreg at Sakase Adtech Co., Ltd. Single-ply composite plate is cured from this prepreg under autoclave environment. The close-up of the material, together with the fundamental dimensions is shown in Fig.1.

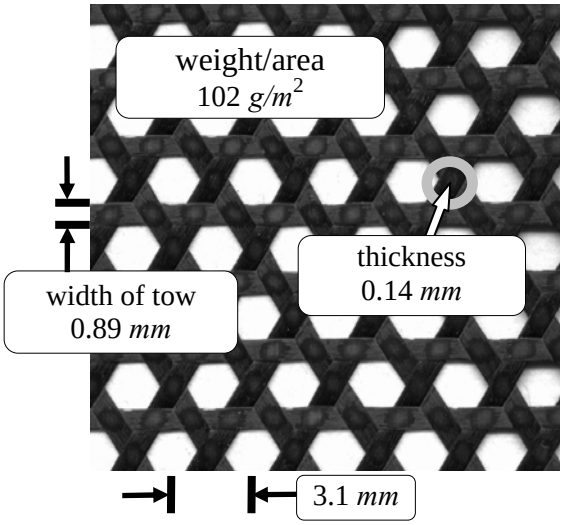

Fig. 1. TWF composite

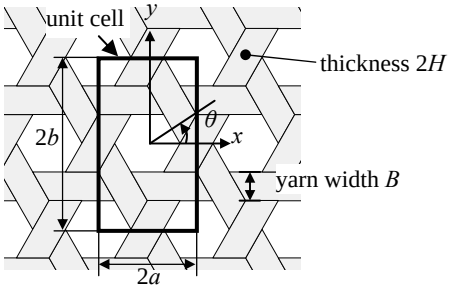

(a) Unit cell region

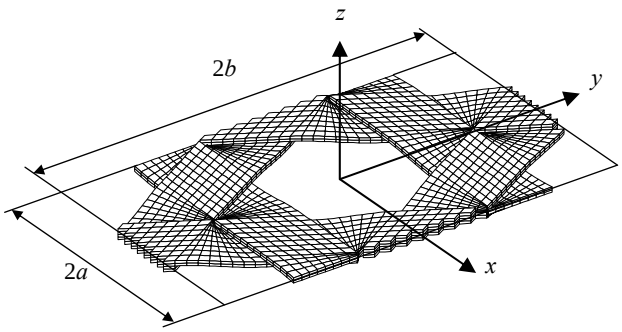

(b) Finite element model

Fig.2. Analytical model of TWF composite

3 Analysis

3.1 Finite Element Analysis

As the TWF composite has periodic nature arising from its fabrication process, unit cell is defined as shown in Fig.2 based on the simplicity when imposing the periodic boundary conditions. Nonlinear finite element analysis is conducted in order to simulate the folding behavior of the composite. Global coordinates x and y are defined as shown in the figure with one of the tow directions coinciding with the x axis. 0^o direction is also defined as that of the x axis. The mechanical properties of the unidirectional tow composite used in the following analyses are shown in Table 1. It should be noted that fiber volume fraction of 76% is used in deriving these properties, though the averaged volume fraction measured from the constituent tows is 63%. This discrepancy is due to the existence of resin rich regions at the surface of the tows.

Table 1. Elastic properties of tow composite used in FE analysis

E_L	E_T	G_{LT}	G_{TT}	ν_{TT}
GPa	*GPa*	*GPa*	*GPa*	
176	17.2	6.86	6.23	0.278

3.2 Results

3.2.1 Initial Stiffness

The initial macroscopic stiffness is first calculated based on the linear finite element analysis combined with the unit cell model. The typical deformed state under bending is shown in Fig. 3. In-plane, coupling and bending stiffness matrices [A], [B], and [D] of the TWF composite are obtained as follows.

$$[A]=\begin{bmatrix}3.04 & 1.80 & 0\\ 1.89 & 3.04 & 0\\ 0 & 0 & 0.619\end{bmatrix}\equiv\begin{bmatrix}A_{11} & A_{12} & 0\\ A_{12} & A_{22} & 0\\ 0 & 0 & A_{33}\end{bmatrix}\quad (1)$$

$$[kN/mm]$$

$$[B]=\begin{bmatrix}0 & 0 & -1.30\\ 0 & 0 & 1.30\\ 1.30 & -1.30 & 0\end{bmatrix}=\begin{bmatrix}0 & 0 & B_{13}\\ 0 & 0 & B_{23}\\ B_{31} & B_{32} & 0\end{bmatrix}\quad (2)$$

$$[N]$$

$$[D]=\begin{bmatrix}1.59 & 0.369 & 0\\ 0.369 & 1.59 & 0\\ 0 & 0 & 0.611\end{bmatrix}\ [N\cdot mm]\quad (3)$$

The components of [*A*] and [*D*] matrices show that the bending stiffness as well as in-plane stiffness exhibits isotropy. These results are consistent with those derived by Kueh and Pllegrino [3] using the beam elements. In addition, the coupling stiffness also exhibits the isotropic nature, as the components satisfy the equation B_{13}=-B_{31}=B_{32}=-B_{23}.

The fictitious laminate of stacking sequence [-60/0/60] that has the same specific weight as the TWF composite is considered. The laminate thickness of this equivalent laminate will be 0.0545*mm*. The stiffness matrices $[A]_{lam}$, $[B]_{lam}$ and $[D]_{lam}$ are calculated to be

$$[A]_{lam}=\begin{bmatrix}4.22 & 1.33 & 0\\ 1.33 & 4.22 & 0\\ 0 & 0 & 1.449\end{bmatrix}\ [kN/mm]\quad (4)$$

$$[B]_{lam}=\begin{bmatrix}0 & 0 & 11.6\\ 0 & 0 & 34.0\\ 11.6 & 34.0 & 0\end{bmatrix}\ [N]\quad (5)$$

$$[D]_{lam}=\begin{bmatrix}0.449 & 0.447 & 0\\ 0.447 & 1.40 & 0\\ 0 & 0 & 0.475\end{bmatrix}\ [N\cdot mm]\quad (6)$$

The in-plane stiffness of the equivalent laminate is higher than that of the original TWF composite, but the bending stiffness of this fictitious laminate exhibits anisotropy, which may introduce additional factors to be considered in design procedures.

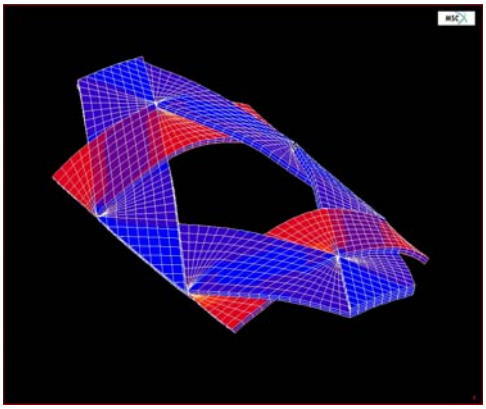

Fig. 3. Deformed state under bending in 0° direction

3.2.2 Nonlinear Behavior

The bending behavior of the TWF composite is shown in Fig.4, in which the results based on linear and nonlinear analyses are both displayed. The unit cell model is again used. The linear analysis bears the identical results for both directions. Bending stiffness in 0° and 90° directions based on nonlinear analysis are almost identical as discussed in the previous section, showing isotropy up to relatively high level of bending curvature. Once the nonlinearity starts to appear, which corresponds to the bending radius of around 5*mm*, the isotopic nature gradually dissipates.

Stresses are also looked into to predict the fracture of the composite. Assuming that the fracture stress is about 2*GPa* for the present base tow composite, the fracture is predicted to take place at bending radius of about 3.5*mm* for both 0° and 90° directions.

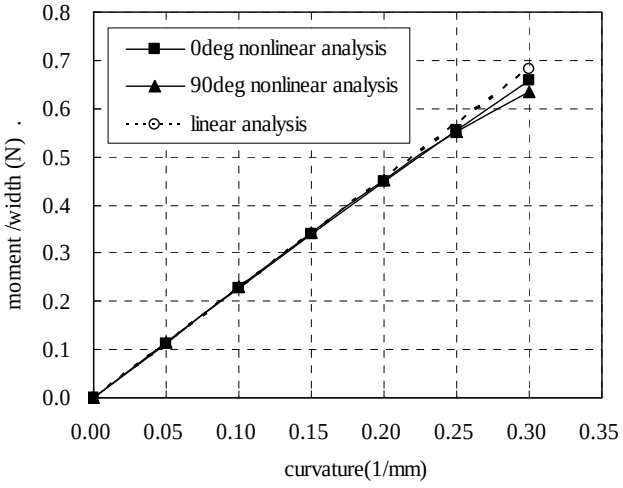

Fig. 4. Analytical prediction of bending behavior

3.3 Effect of Specimen Width

As shown in the previous work [2] under the case of tensile loading, the apparent stiffness of the material depends on the width of the specimen or the model used. The bending stiffness is calculated herein by introducing finite element models representing different types of specimen configurations. The model is made up of appropriate number of unit cell models that are connected side by side. The bending stiffness plotted for the various values of specimen width is summarized in Fig.5. The abscissa is the inverse of the specimen width, zero corresponding to the infinite plate. Stiffness in both 0^o- and 90^o- directions converge to an identical value which can be predicted from the unit cell model. Thus care should be taken when estimating the stiffness especially for the components of small size relative to the unit cell dimensions.

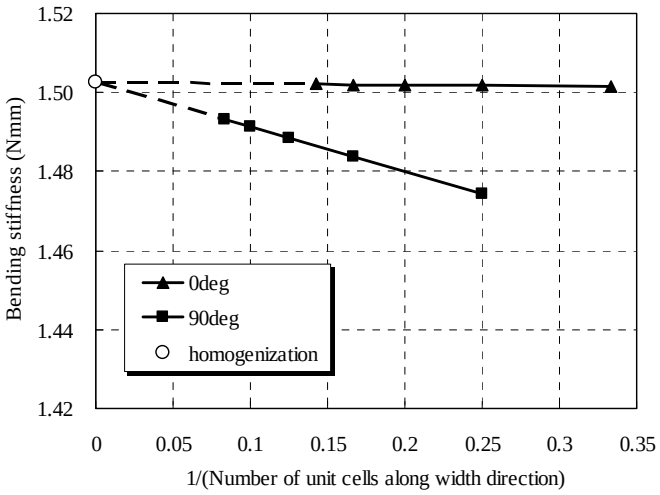

Fig. 5. Effect of specimen width on bending stiffness

4 Pure Bending Experiment

4.1 Setup

Three point bending test was conducted in the previous work [4], which was found to be insufficient for the measurement under large curvatures. Thus pure bending test is conducted based on the apparatus used to measure the properties of papers [5]. The specimens are 100*mm* long and 16*mm* wide. The experimental setup is schematically shown in Fig.6. Components A and B in the figure can rotate freely and transform the load *F* to the pure bending moments that are conveyed to the specimen ends. The component A is attached to the arm which can swing around point O to conform with the specimen deflection. The specimen and the apparatus under loading is shown in Fig.7.

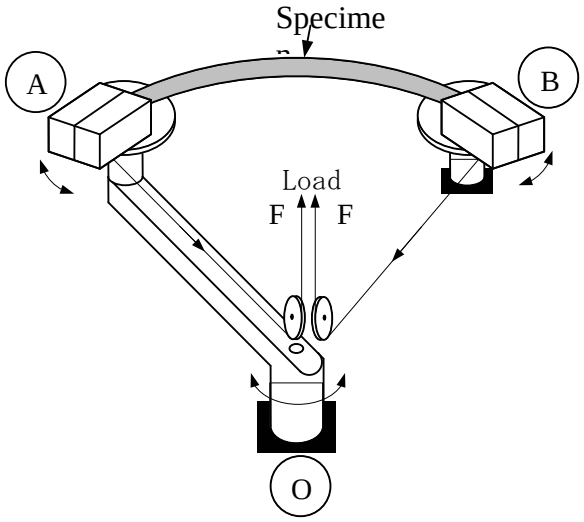

Fig. 6. Schematic of experimental setup for the pure bending test

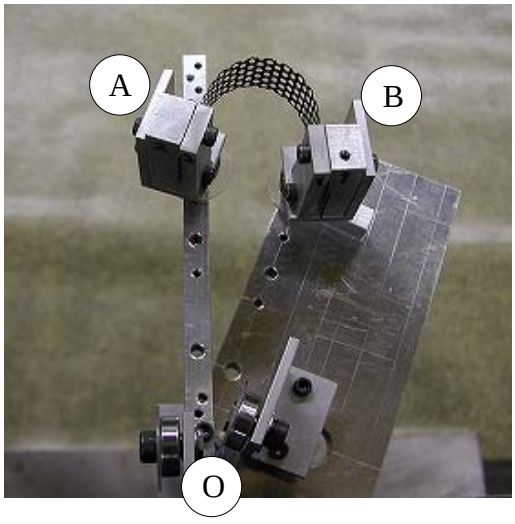

Fig. 7. Pure bending test

4.2 Results

The bending moment versus curvature relation obtained from the pure bending test is shown in Fig.8. The bending moment is normalized by the

width of the specimens. The experimental results are limited to relatively lower curvature level compared to the analytical results in Fig. 4. The values of initial stiffness in both directions coincide well, and are in good agreement with the analytical results. However the nonlinear softening effects show up at lower curvature levels than the analytically predicted results. These softening tendencies may be the contributions of the resin rich regions lying between the tows at their intersections. The slightly lower stiffness for 90^o specimen is observed at higher curvature, and this is consistent with the analytical predictions as well as the experimental results of reference [6]. The unloading path shows almost identical trends for specimens in both directions in the curvature range of up to $0.06(1/mm)$ corresponding to the radius of curvature of $17mm$. The example of the loading and unloading behavior is shown in Fig. 9 for 90^o specimen. This fact confirms the tenacious characteristic of the TWF composite for flexural use.

Additionally conducted crush bending tests showed that the radius went down to $2\sim3mm$ prior to the detection of the major failure for both specimens. Example of the crushing test is shown in Fig. 10.

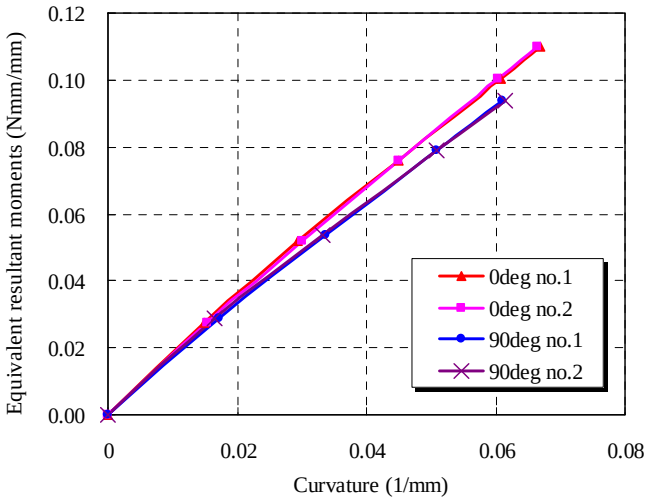

Fig. 8. Moment vs. curvature relationship from pure bending test

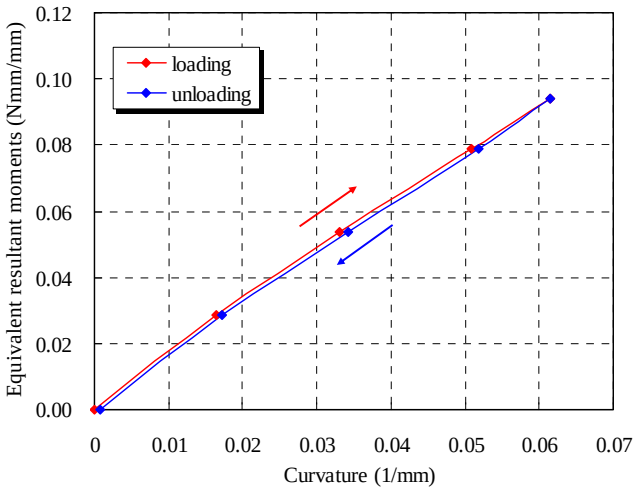

Fig. 9. Loading-unloading in pure bending test (90^o-direction)

Fig. 10. Crushing test

5 Thermal Expansion Measurement

5.1 Setup

Thermal expansion test is conducted using the transparent glass plates installed with the heating films. Thermo-couples and a set of two Laser/CCD extensometer measuring systems are used for temperature and displacement measurements. Thermocouples are attached to the glass heating system as well as to the specimens showing no significant difference in the temperature measurements. Experimental setup is shown in Fig.11. Several types of temperature cycles are adopted in the range of 20 to 100 ^oC. The temperature is controlled by the PID feedback

system. The gap between the top and bottom glass heating system are set to 3*mm* by inserting paper strips of equal thickness to the edges of the plates. Rectangular specimens of 60*mm* by 95*mm* are used in the experiment. One of the shorter side edges of the specimen is clamped so that there will be no undesired rigid rotational displacement. The measuring system is first verified with the aluminum sheet to obtain the thermal expansion coefficient of the known material. The measurements are conducted at least twice to verify the reproducibility of the results.

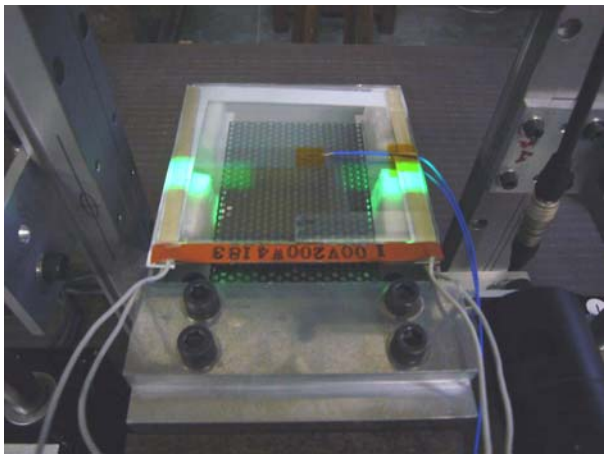

Fig. 11. Experimental setup for coefficient of thermal expansion measurement

5.2 Results

The results from thermal expansion test are shown in Fig.12. The factors that affect the measurement results are the restraint conditions of the specimens and the thermal loading rate. The reproducibility of the experimental results show that constraining one edge of the specimens gives the most reliable results compared to the experiments under free or point constraint conditions. The increasing and decreasing rates of temperature change are also altered in several ways to examine the results. The continuous as well as step change in temperature has been tested, where the step change in temperature is used to obtain the results shown in Fig.12. The temperature is increased and decreased by steps of 20*K* and is held at each stage for 30*min*. This is supposed to be enough as further temperature holding exhibited no apparent change in the results. However there are considerable amounts of hysteresis observed in the results, which are reproducible under multiple thermal cycles. Average thermal expansion coefficients derived from the strains under temperature rising process are $\alpha_0=2.9*10^{-6}(1/K)$ for 0^o specimens and $\alpha_{90}=3.2*10^{-6}(1/K)$ for 90^o specimens. These were higher than the results previously obtained from the preliminary results [2] of $\alpha_0=\alpha_{90}=1.14*10^{-6}(1/K)$. It should be noted that the edge effect cannot be eliminated using the present experimental apparatus which measures the displacements at the edges of the specimen. This may possibly be part of the cause of the discrepancy between two directions.

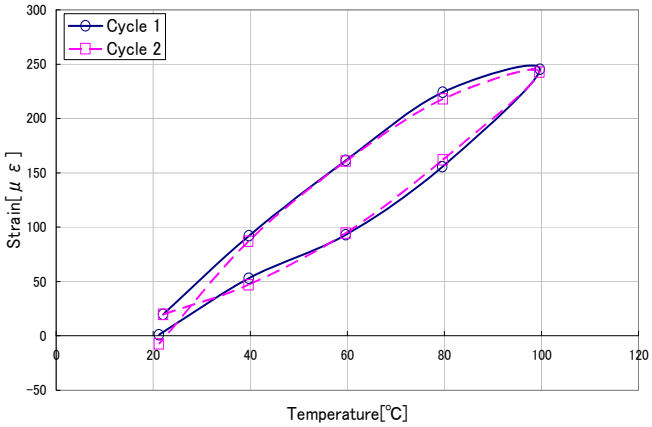

(a) 0^o-direction

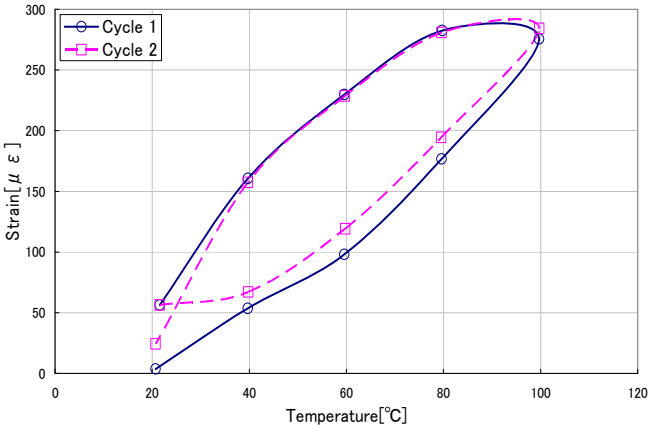

(b) 90^o-direction

Fig. 12. Strain measurement under thermal loading

6 Conclusions

In the light of applying the tri-axially woven fabric composites to deployable space structures, the bending characteristics of the material system are analytically and experimentally investigated. The stiffness isotropy previously observed under tensile loading is shown to hold as well under the flexural loading based on the linear analysis combined with the assumption of infinite size specimens. The effect of specimen width shows up as well under bending analysis. The anisotropy that emerges at high loading levels under tensile load is predicted to be not as salient under the flexural loading. To verify the analytical predictions, pure bending test is employed. The experimental results support the predicted isotropy for infinite plates, though the actual specimens are of finite width. Thermal expansion test is also conducted to experimentally obtain the thermal expansion coefficients, which are found to be larger than that predicted previously through the analysis. The overall isotropic nature as well as the excellent flexural strength of the TWF indicates that the material system is one of the potent candidates for various components of light-weight deployable structures, especially in space use.

References

[1] Yoshida, K. and Aoki, T., "Tensile behavior of 2-D triaxially woven fabric composite." Paper 166, *Proceedings of the American Society for Composites 18th Technical Conference*, 2004.

[2] Yoshida, K. and Aoki, T., "Mechanical and thermal behaviors of triaxially-woven carbon/epoxy fabric composite." Paper 2006-1688, *Proceedings of the 47th AIAA/ASME/ASCE/AHS/ASC Structures, Structural Dynamics, and Materials Conference*, Rhode Island, 2006.

[3] Kueh, A.B.H. and Pellegrino, S., "ABD matrix of single-ply triaxially weave fabric composites." Paper AIAA-2007-2161, *Proceedings of the 48th AIAA/ASME/ASCE/AHS/ASC Structures, Structural Dynamics, and Materials Conference*, Hawaii, 2007.

[4] Aoki, T, Yoshida, K. and Watanabe, A., "Feasibility study of triaxially-woven fabric composite for deployable structures." Paper AIAA-2007-1811, *Proceedings of the 48th AIAA/ASME/ASCE/AHS/ASC Structures, Structural Dynamics, and Materials Conference*, Hawaii, 2007.

[5] Fellers, C. and Carlsson, L., "Measuring the pure bending properties of paper." *Tappi*, Vol. 62, No. 8, pp.107-109, 1979.

[6] Kueh, A., Soykasap, O. and Pellegrino, S., "Thermo-mechanical behaviour of single-ply triaxial weave carbon fibre reinforced plastic." *Proceedings of the European Conference on Spacecraft Structures, Materials and Mechanical Testing 2005*, pp.1465-1474, 2005.